Springer

KSME

Journal of Mechanical Science and Technology 24 (6) (2010) 1245~1254
www.springerlink.com/content/1738-494x
DOI 10.1007/s12206-010-0340-5

Experimental and numerical assessment of the improvement of the load-carrying capacities of butterfly-shaped coupling components in composite structures †

Gürkan Altan* and Muzaffer Topçu

Faculty of Engineering, Department of Mechanical Engineering, Pamukkale University, Kınıklı 20070 Denizli, Turkey

(Manuscript Received June 1, 2009; Revised January 20, 2010; Accepted January 29, 2010)

Abstract

This study was designed to analyze the load-carrying capacities of composite structures connected face-to-face by a butterfly coupling component experimentally and numerically without adhesive. The results of the experimental studies were supported with numerical analysis. In addition, the butterfly coupling component was developed geometrically with a view to the results of the numerical and experimental studies. The change in the load-carrying capacity of the improved butterfly coupling components was analyzed numerically and experimentally to obtain new results. Half-specimens and butterfly-shaped lock components were cut with a water jet machine. Experiments and analyses were conducted to analyze the effects of coupling geometry parameters, such as the ratio of the butterfly end width to the specimen width (w/b), the ratio of the butterfly middle width to the butterfly end width (x/w), and the ratio of the butterfly half height to the specimen width (y/b). It was intended to determine the damage in the butterfly before any damage to the composite structure and to increase the service-life span of the composite structure with the repair of the butterfly lock. As a result of this study, it was determined that the geometrical fixed ratios (w/b) and (x/w) were 0.4 and 0.2 at 0.4 of (y/b) according to the experimental and numerical studies with basic and modified models.

Keywords: Butterfly joint; Failure load

1. Introduction

The use of composite materials in various fields of application has rapidly increased due to their resistance to corrosion and their lightness. These characteristics have led designers to attempt to design proper joint types for these materials. The most important problem with composite structure designs is the strength weakness in the sites of the composite joint. Therefore, studying the type, load, and starting direction of the damage is important in designing joining sites of the composite structures. Load behaviors of the jointed composite structures, as well as the designs and ways of joining them, have been investigated both numerically and experimentally by a number of researchers.

Composite structures are usually jointed mechanically and/or by adhesive. Mechanical joints are often made in the shape of a single or double overlapping joint with a bolt or a rivet. There are three different modes of damage in mechanically jointed composite structures: net tension, shear out, and bearing [1, 2]. These types of damage can be seen simultaneously. In net-tension and shear-out damages, force suddenly decreases when the damage occurs. In bearing damage, however, the force decreases slowly when the maximum load that can be carried by the composite structure is reached. Therefore, the designer should create the optimum geometric design to prevent sudden damage. The joining of composite structures by adhesive can be achieved with various designs, such as lapping and butt [3-7]. The load-carrying capacity is affected by factors such as whether the adhesive to be used can adapt well to the composite structure, the type of the joining geometry, and thickness of adhesive. An adhesive joint can be subjected to loadings such as net tension, shear out, or peeling. The strength of the adhesives to the distributions of stress caused by the effect of peeling is weak, while their strength to the distributions of stress caused by the loads of tension and shear-out is strong [8-10]. Bahei-El-Din and Dvorak [11] examined the strength of new joint designs for adhesive bonding of thick multilayered composite adherents through finite-element computations. Grassi et al. [12] presented a simple and efficient computational approach for analyzing the benefits of through-thickness pins for restricting debond failure in joints. Aktas and Dirikolu [13] carried out an experimental

† This paper was recommended for publication in revised form by Associate Editor Chongdu Cho

*Corresponding author. Tel.: +90 258 296 3163, Fax.: +90 258 296 3262
E-mail address: gurkanaltan@pau.edu.tr

and numerical study to investigate the strength of a pinned-joint carbon epoxy composite plate. Zeng and Sun [14] investigated the performance of wavy-lap joint under cyclic tension-tension loading conditions. They performed geometrically non-linear two-dimensional elastic analyses to obtain an understanding of the experimental results using commercial code Abaqus.

In this study, new mechanical butt joints made with a butterfly coupling component are used as an alternate to adhesively bonded face-to-face or butt joints. The results of the experimental studies are supported with numerical analysis. Moreover, the butterfly coupling component has been developed geometrically in consideration of the results of numerical and experimental studies. The change in load-carrying capacity of the developed butterfly coupling components has been analyzed numerically and experimentally, and the new results obtained are presented. Butterfly-shaped coupling components are used with the tight insertion method to connect the composite plates face-to-face.

2. Manufacturing the material and its mechanical properties

In this study, glass fiber-epoxy composite material was used in the experiments. The glass fiber-epoxy composite material used was manufactured by the firm Izoreel Composite Isolate Materials through hot pressing**.** The order of the glass fiber was chosen to be unidirectional. The epoxy resin used as the material of matrix consisted of a mixture of 100/80 Ciba Geigy, Bisphenol A, CY-225 epoxy, and Ciba Geigy, Anhydride, HY-225 hardener. As seen in Fig. 1, the unidirectional glass fiber with a weight of 270 g/m^2, which can be obtained from the market in the shape of roller, was cut to produce 1000x500 mm cloths that can be used to create the layers of layered-composite plate. Glass fiber cloth of the same dimensions was cut according to the number of layers of each composite plate.

After the cutting of glass fibers in the shape of the cloth, the mixture of epoxy resin, which is the matrix material, was prepared. The prepared mixture of fluid epoxy resin and hardener was saturated onto each 1000x500 mm piece glass fiber cloth. The cloth was placed on the mould by means of a roller. In this way, epoxy resin was applied to each glass fiber layer and a 16-layer wet composite material was obtained in the mould. The wet material was then hot-pressed so that it can be cured and reach minimum thickness. Pressing was conducted to better saturate the epoxy resin onto the glass fiber cloth and eliminate air bubbles for the probable interface gaps. The glass fiber-epoxy composite material was cured under 14 MPa pressure at a temperature of 120° C. The material was pressed at this temperature for 2 h. The composite plate with 16 layers was removed from the press and left to cool to room temperature. The thickness of the composite plate was reduced to 3.5 mm after trimming. Composite plates of standard thickness were also produced via the same treatment to determine the mechanical properties of the composite material.

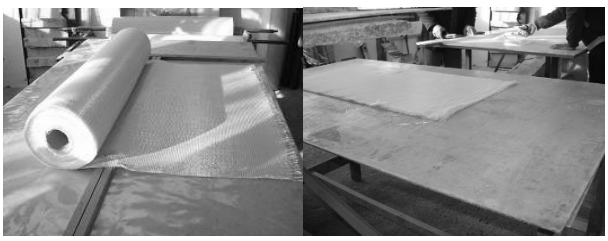

Fig. 1. Unidirectional glass fiber.

The mechanical properties of the glass fiber-epoxy composite material were determined according to ASTM standards under the loads of tension, compression, and in-plane shear. Experiments were conducted thrice, and their average values were taken into consideration. As the composite plate is made of unidirectional glass fiber cloth, its mechanical properties changed in two different ways. The direction to the fiber was accepted as Direction (1), while the one perpendicular to the fiber as Direction (2). The mechanical properties of the composite plate on the 1-2 planes were obtained using three specimens for each mechanical property, and the average properties were determined. Fig. 2 shows examples of the specimens.

The experiments for the determination of the mechanical properties were conducted at 23±1° C room temperature and 50%±10 relative humidity according to ASTM standards. The experiments were conducted using the tension test machine with 50 kN capacity. Tension properties such as longitudinal modulus (E_1), transversal modulus (E_2), Poisson ratio (ν_{12}), longitudinal tension strength (X_t), and transversal tension strength (Y_t) were measured with static tension according to ASTM D3039-76 [15] standard test method. Compression properties such as longitudinal compression strength (X_c) and transversal compression strength (Y_c) were measured from the unidirectional specimens using static compression according to ASTM D3410-75 [16] standard test method. An important factor to consider in determining the in-plane shear strength properties is that pure in-plane shear stress is enabled at the measuring site of the specimen [17]. The Iosipescu in-plane

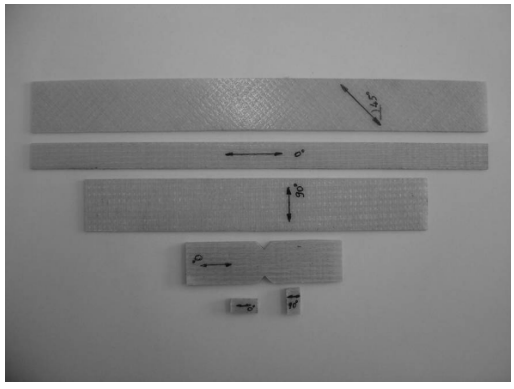

Fig. 2. Specimens for mechanical properties of the glass fiber-epoxy composite material.

Table 1. Mechanical properties of the glass fiber-epoxy composite material.

E_1 (MPa)	E_2 (MPa)	G_{12} (MPa)	ν_{12}	X_t (MPa)	Y_t (MPa)	X_c (MPa)	Y_c (MPa)	S (MPa)
44150	12300	4096	0.20	775	130	305	80	95

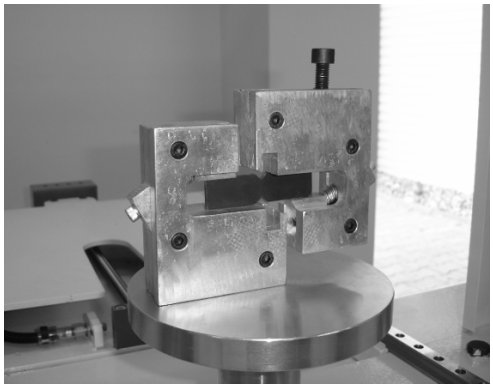

Fig. 3. Iosipescu loading apparatus.

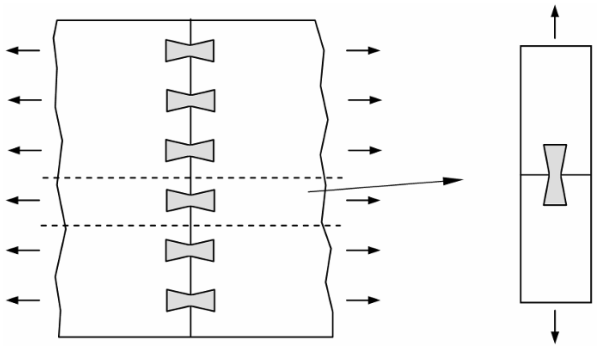

Fig. 4. Type of butterfly joint.

Fig. 5. Cutting specimens using water jet.

shear test method was used to determine the in-plane shear strength (S) according to ASTM D5379 [18] standard test method. To detect the in-plane shear strength (S) in the composite structures, Iosipescu loading apparatus was created according to ASTM D 5379 standard (shown in Fig. 3).

Shear modulus (G_{12}) was determined using the specimens with a main axis as 45° according to ASTM D3518-76 [19] standard test method. It was calculated by measuring the strains in the direction of tension [20]. The mechanical properties of the composite material as determined from the experiments are given in Table 1.

All the specimens used in the experiments were taken from the manufactured composite plate. The material of the composite butterfly used in the experiments is the same as those of the composite half-specimens.

3. Experimental and numerical method

In this study, butterfly-shaped coupling components were used to join the composite plates face-to-face using the tight insertion method. As shown in Fig. 4, specimens were taken from the composite plates that were mechanically joined face-to-face, and experiments were conducted. The effects of the change in the geometric parameters of the butterfly-shaped coupling components on the maximum load-carrying capacity were analyzed, and several improvements were made in the butterfly geometry.

All the specimens used in the experiments were cut with water jet from the composite plates manufactured at the Zümrüt Glass firm according to the approved geometric parameters and by ASTM standards. The error of cutting that may arise due to the use of the water jet (as the method of cutting and the amount of temperature that may occur during the process of cutting) was either reduced to minimum levels or eliminated. Fig. 5 shows an example of creating specimens using water jet.

The dimensions of the specimen as seen in Fig. 6 are as follows: sample width (b) = 40 mm, specimen total length (L) = 180 mm, and sample thickness (t) = 3.5 mm. With the main dimensions of the specimen jointed face-to-face (b, L, t) kept fixed, the end width (w), middle width (x), and half-length (y) of the butterfly lock were changed.

In a study by Topçu et al., a number of experiments were conducted to observe the effects of the geometric parameters of butterfly joints on the loads of damage. These experiments were conducted by changing the ratio of butterfly end width to the specimen width (w/b) and the ratio of butterfly middle width to the butterfly end width (x/w) from 0.2 to 0.8. In their experiments, the ratio of butterfly half-length to the specimen width (y/b) was changed to 0.2, 0.4, and 0.6. From their experimental study, they determined that the ratio of butterfly end width to specimen width (w/b) was 0.4, the ratio of butterfly middle width to the butterfly end width (x/w) was 0.2, and the ratio of butterfly half-length to the specimen width (y/b) was 0.4 [21]. In the present study, the numerical analysis of the best butterfly joint determined by Topçu et al. was first made using the software Abaqus 6.8, one of the finite-element method package programs. To compare the distributions of stress obtained from the numerical analyses with each other, the analyses in this study was conducted under a fixed load and similar conditions. Instead of conducting numerical analyses of all the geometric changes, the numerical analysis of the change in (w/b) ratio when (x/w) ratio was 0.2 was conducted and the change in (x/w) ratio when (w/b) is 0.4 was analyzed numerically in the determined butterfly half-length. Table II presents the dimensions of butterfly coupling components to be used in the numerical analysis.

In the present study, new joint systems were created with

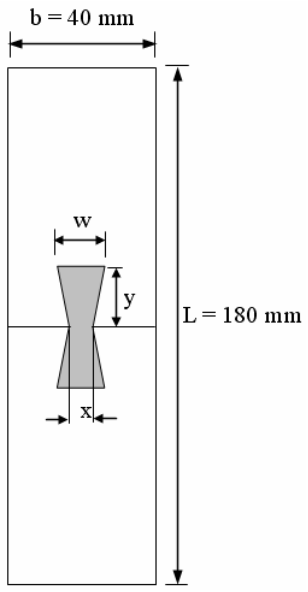

Fig. 6. Dimensions of the specimen.

slight geometric changes by generally maintaining the best butterfly joint geometry obtained with the finite-element method. The butterfly end width (w) of the best butterfly coupling component chosen here was 16 mm, the butterfly middle width (x) was 3.2 mm, and the butterfly half-length (y) was 16 mm. The chosen and newly made butterfly joints are shown in Fig. 7. The butterfly coupling component used in the coupling shown in Fig. 7(a) was the best cornered butterfly coupling component determined as a result of the experiments made by Topçu and others. This type of butterfly was taken as the basic model. In the joint shown in Fig. 7(b), the end corners of the butterfly were rounded to have a 2 mm radius. This type of butterfly was named the rounded model. The rounded butterfly coupling component shown in Fig. 7(c) was also reinforced with 2 mm-wide rods from its sides. This type of butterfly was named the reinforced model. Both the end corners of the butterfly were rounded, and the sloping side surfaces of the butterfly model shown in Fig. 7(d) were designed as parabolic. This type of butterfly was named the sandglass model. Half-specimens were mechanically jointed using the tight insertion method with the cut butterfly coupling components. Load-carrying capacities of the improved joint specimens were obtained from the tension test machine with 50 kN load capacity. All the specimens were loaded at the fixed tension speed of 1 mm/min. The experiments were repeated three times for each value. Experiments with faulty results were repeated. The experiment was ended when any amount of decrease in the applied load was observed. The load of damage in the specimen occurred in the first fall in the load applied. Thus, maximum damage loads for each model were determined. When the applied load reached the specimen damage load, damage fractures were observed to have begun to occur either in the composite butterfly or in the composite structure around the butterfly. To understand the shapes of the

Table 2. Dimensions of butterfly coupling components.

Dimension (mm)	Change in (x/w) ratio when (w/b) ratio is 0.4				Change in (w/b) ratio when (x/w) ratio is 0.2			
	0.2	0.4	0.6	0.8	0.2	0.4	0.6	0.8
w	16	16	16	16	8	16	24	32
x	3.2	6.4	9.6	12.8	3.2	3.2	3.2	3.2
y	16	16	16	16	16	16	16	16

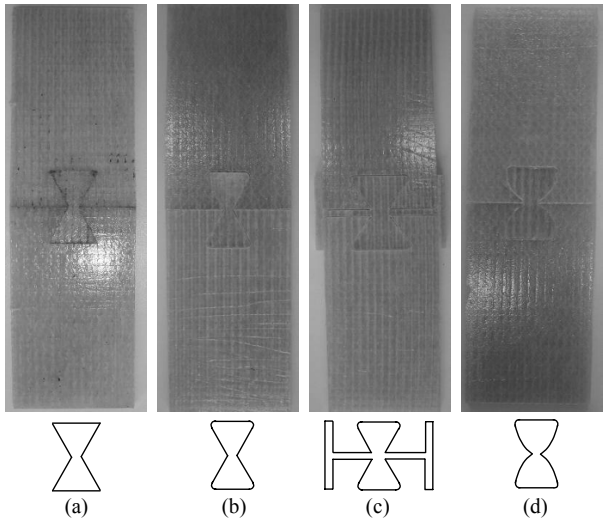

Fig. 7. The improved butterfly geometry: (a) basic model; (b) rounded model; (c) reinforced model; (d) sandglass model.

damage, experiments on some specimens were continued until their last damage. In this way, the effects of the improved butterfly geometry could be analyzed.

Load-carrying capacities of the same composite half-specimens that may occur when they are jointed with two butterfly coupling components positioned side by side were also analyzed. Since the specimen width was fixed as 40 mm, butterfly end width (w) of the basic butterfly model was reduced to half by keeping the butterfly middle width (x) as fixed. Fig. 8 presents an example for the double butterfly joint. Damage loads of the single and double joints made at the same butterfly dimensions were experimentally found and compared for different butterfly half-lengths.

Abaqus 6.8 package program was used in the numerical analysis conducted with the finite-elements method. Three-dimensional models of the specimens jointed with the butterfly coupling component were created. As the geometries of the butterfly coupling components were altered, knowing the stresses on the butterfly and determining the sites of probable damage is crucial for the safety of the structure. Therefore, a firmer network of solution was created for the butterfly coupling components than the half-specimens. To compare the distributions of stress in butterfly joints of various geometries, as shown in Fig. 9, two stress distributions were tackled on the same line, one being through the butterfly middle axis (Way 1) and the other from the site of the half-specimen near the butterfly (Way 2).

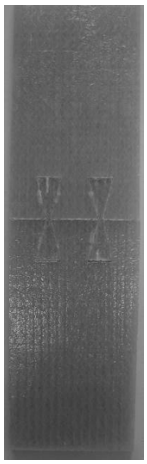

Fig. 8. Double butterfly joint.

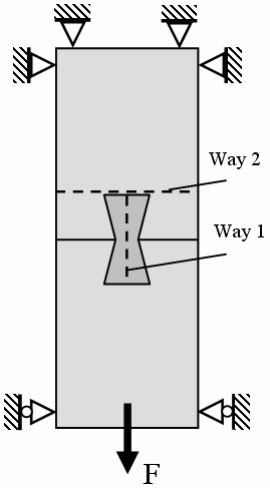

Fig. 9. Ways of the stress distribution in the numerical analysis.

4. Results and discussions

Butterfly-shaped lock and half-specimens used in the experiment specimens mechanically jointed face-to-face were cut and taken from the $[0]_{16}$ orientation-composite plate. The present study experimentally and numerically investigated the occurrence of the change in the load-carrying capacities of the specimens as well as the change in the geometric parameters of the butterfly coupling components and model.

To determine the accuracy of the conducted stress analysis, experimental and numerical study results were analyzed and compared. Only the obtained numerical and experimental butterfly displacements were compared. The load value used in the finite element method program for determining the load carrying capacity and the failure shapes from stress analysis was chosen as 800 N. From the experiments, it was determined that butterfly damages do not occur at this load value. The comparison of the total butterfly displacements obtained from the experimental and numerical studies are shown in Fig. 10. The results obtained from the experimental and numerical studies were very close; therefore, both of these studies were found to support each other.

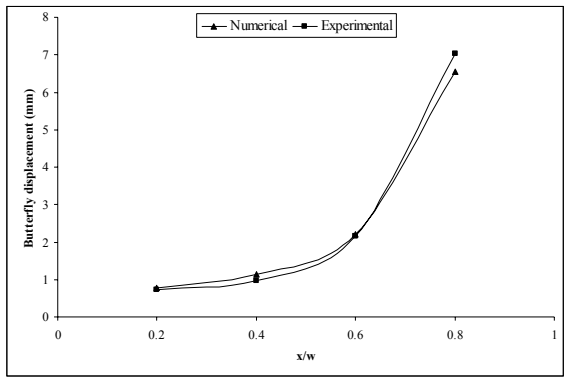

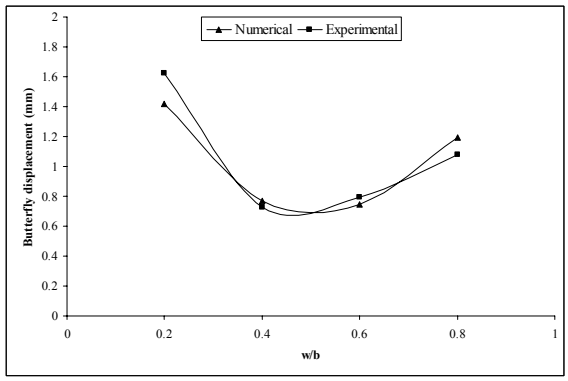

Fig. 10. The comparison of the butterfly displacements with experimental results and finite element method results.

Fig. 11(a) shows the changes in the load-carrying capacities of the specimens made with the butterfly coupling components at the fixed ratio of w/b= 0.4 for the butterfly half-length (y) of 16 cm according to the (x/w) ratios. Fig. 11(b) shows the change in the damage loads according to the (w/b) ratio of the experiment specimens at the fixed ratio of x/w= 0.2. The joint experiments determined that the damage occurs more on the corners on the butterfly. This ensures that the damage occurring on the butterfly can be seen before the composite structure is totally damaged, and the service life of the composite structure can be increased with the change in the butterfly coupling component [21]. The results obtained experimentally were assessed with the stress distributions obtained with the numerical analysis under the same conditions and the fixed load.

Stress distributions of the butterfly joints at different ratios of (x/w) and a fixed (w/b) ratio of 0.4 are shown in Fig. 12. The value of load used in the analysis to determine the kinds of damage that may occur and the load-carrying capacities by means of the stress analysis was chosen from the load values in which butterfly joints have not been damaged. Stress values obtained from the stress analysis made under the same load were obtained as being different due to the different butterfly geometries. It was determined that ultimate stress obtained in Fig. 12(a) was the lowest, while the one in Fig. 12(d) with the increase in the (x/w) value with ultimate stress values was the highest. Viewed generally, ultimate stresses were observed to

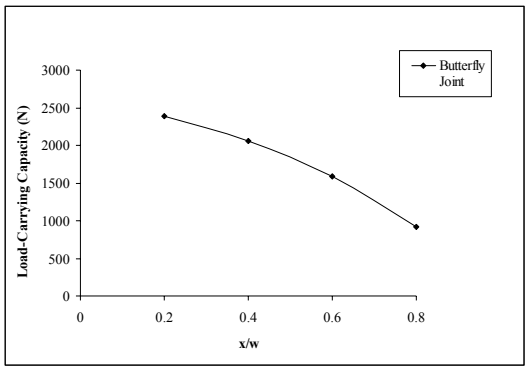

(a)

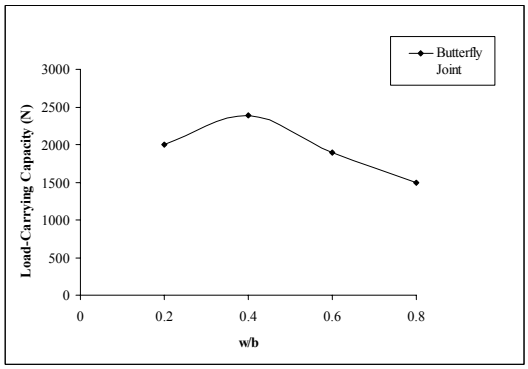

(b)

Fig. 11. The ratios of geometrical parameters versus load-carrying capacities.

occur on the butterfly coupling components. Any damage that may occur on the damage loads is expected to occur where the ultimate stress occurs. For that reason, butterfly coupling components may be accepted as the initial sites of damage.

Since the stresses occurring on the butterfly coupling component with the increase in the (x/w) ratio are concentrated towards the corners, the butterfly cannot lock both half-specimens exactly, and any probable damage should occur on the butterfly corners. The load-carrying capacities of the specimens with composite butterfly are thought to be at maximum because they are locked more when (x/w) ratio is equal to 0.2. The fall in the maximum load-carrying capacities with the increase in (x/w) ratio points to the importance of the butterfly middle width. With the increase in the butterfly middle width, the shape of the butterfly coupling component approaches square or rectangular. Therefore, there appears to be a fall in its load-carrying capacity as the butterfly coupling component begins to lose its capacity for locking. Due to the fact that it becomes square or rectangular when (x/w) ratio is equal to 1, the butterfly coupling component cannot carry load. In this case, adhesive techniques should be used to make a joint.

The stress values occurring at the fixed w/b ratio of 0.4 and along the butterfly axis (Way 1) are shown in Fig. 13. Ultimate stress values occurred on both ends due to the geometry

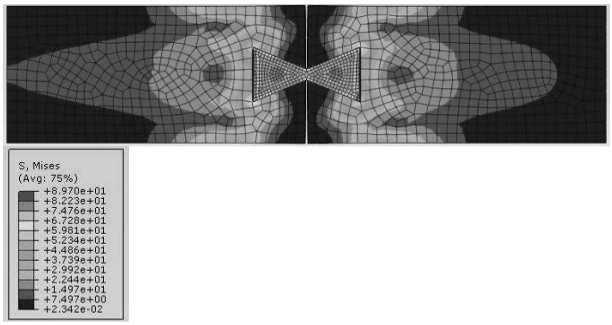

(a) x/w=0.2

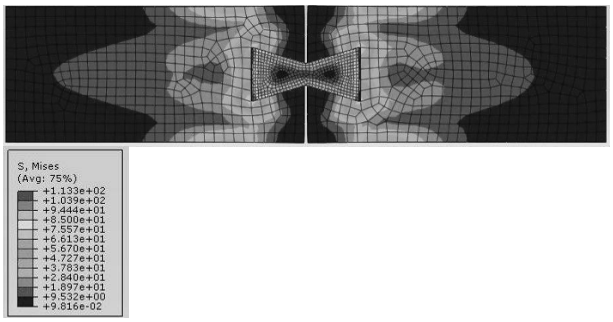

(b) x/w=0.4

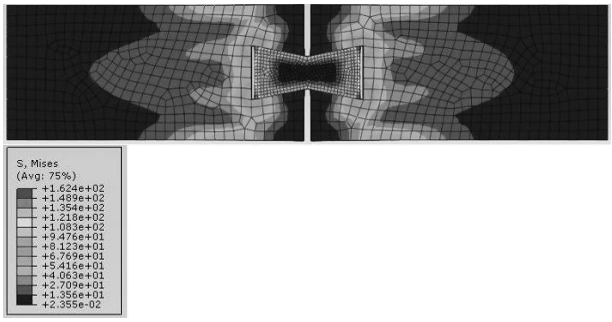

(c) x/w=0.6

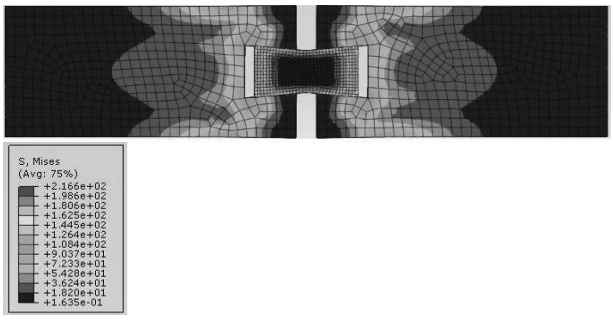

(d) x/w=0.8

Fig. 12. Stress analysis with Abaqus program at the different ratios of (x/w) and at the fixed (w/b) ratio of 0.4.

of the butterfly. However, in the narrowing middle sites of the butterfly coupling component, stress values were observed to be much lower than in the end sites. The sites of ultimate stress obtained under the same loads indicate probable damaged sites. Therefore, this case showed that damage occurs from the corners of the butterfly coupling component first. When (x/w) ratio is 0.2, stress values obtained from the middle part of the butterfly coupling component are higher than

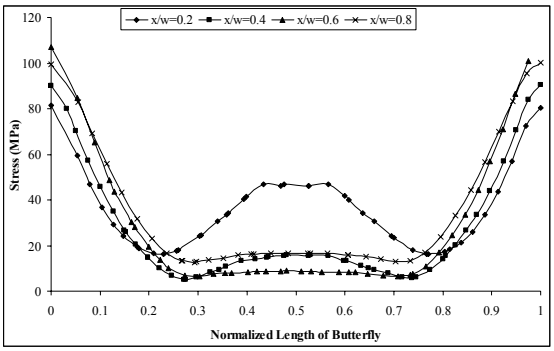

Fig. 13. The stress values occurring at the fixed w/b ratio of 0.4 and along the butterfly axis (Way 1).

the other values of the (x/w) ratio. This case shows that the load transferred over half-specimens is conveyed not only through the sloping side surfaces of the butterfly coupling component, but also through the butterfly middle width. In other words, when the ratio of butterfly end width to butterfly middle width is 0.2, the specimens are locked in the best way and maximum load transfer is realized.

Stress analysis of the different (w/b) ratio changes at the fixed (x/w) ratio of 0.2 is shown in Fig. 14. Different stress values were obtained from the stress analysis under the same load due to the different butterfly geometries. The joints in which maximum stress sites were only on the butterfly were obtained, as seen in Fig. 14 (a) and (b), when the (w/b) ratio was 0.2 and 0.4. When the stress values were compared, it was determined that stress values obtained with the w/b ratio of 0.2 were higher than those with the w/b ratio of 0.4. Thus, the joint with the w/b ratio of 0.4 is expected to be damaged later than the one with the w/b ratio of 0.2. The joints in which ultimate stress sites were on the butterfly coupling component and the specimen were obtained, as seen in Fig. 14 (c) and (d), when the w/b ratio was 0.6 and 0.8. Accordingly, ultimate stress sites occurred in the butterfly end sites, in the sites on the specimen near the butterfly end parts (Fig. 14 (c)), and in the sites on the specimen near the butterfly end parts, as shown in Fig. 14 (d). These account for the fall in damage load obtained in the experiments. It was determined that half-specimens can be damaged because the parts of the butterfly coupling components that held the butterfly lock parted in the half-specimens when w/b ratio is 0.6 and 0.8. If the x/w ratio is 0.2, the load-carrying capacity of the composite butterfly specimens will be the maximum when w/b ratio is 0.4. Thus, it is apparent that the choice of the butterfly end width is rather important for the load-carrying capacity.

The stress values along the specimen width near the end side of the butterfly coupling component (Way 2) are given in Fig. 15. The stress values in the zones on the half-specimens near the butterfly end sides were much higher than the ones obtained along Way 2. As the butterfly joint in which these top maximum stress values are in the minimum values are damaged later, its load-carrying capacity are higher than the type of joint made with the w/b ratio of 0.4.

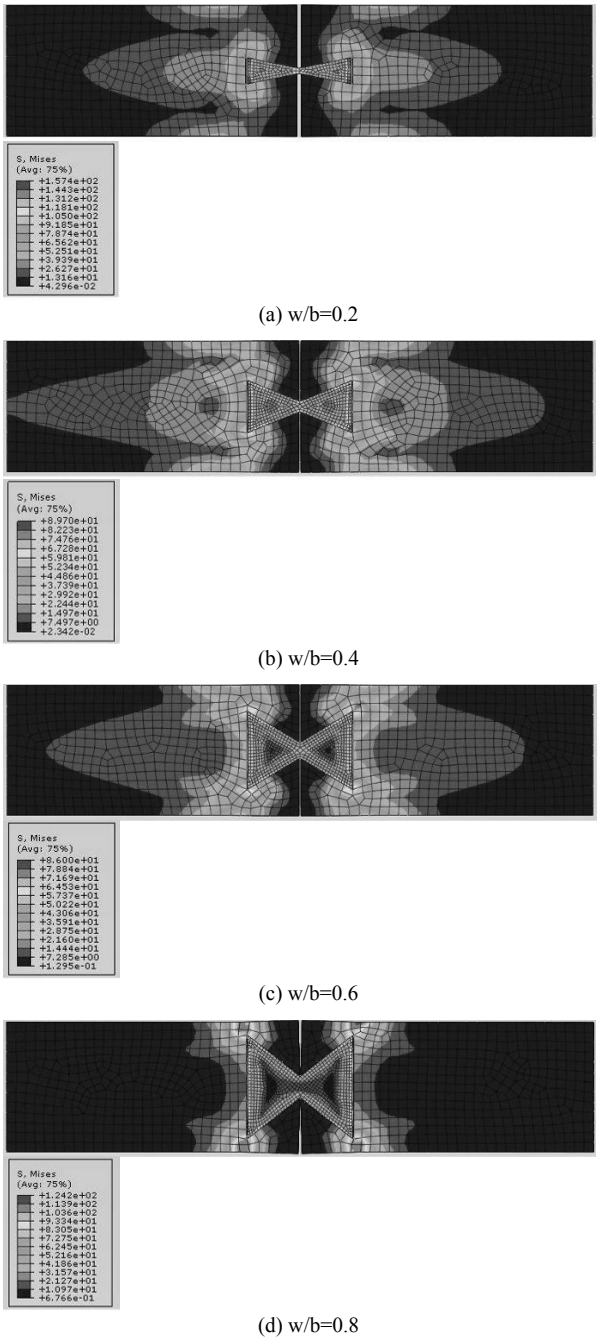

(a) w/b=0.2

(b) w/b=0.4

(c) w/b=0.6

(d) w/b=0.8

Fig. 14. Stress analysis with Abaqus program at the different ratios of (w/b) and at the fixed (x/w) ratio of 0.2.

According to the data from the stress analysis and experiments, the joint specimens made with the (x/w) ratio of 0.2 and (w/b) ratio of 0.4 had the maximum load-carrying capacities. Accordingly, the shape of the butterfly coupling component at the fixed (x/w) ratio of 0.2 was improved to obtain higher load-carrying capacities. The defined angled butterfly coupling component was taken as the basic model. The samples whose geometry were developed from this basic model were named rounded, reinforced, and sandglass models, respectively. The changes in the load-carrying capacities of the

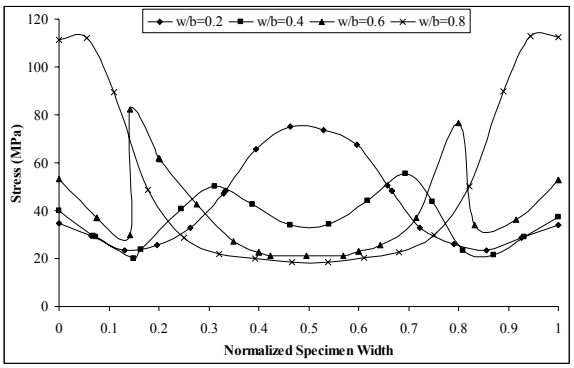

Fig. 15. The stress values along the specimen width (Way 2) at x/w =0.2.

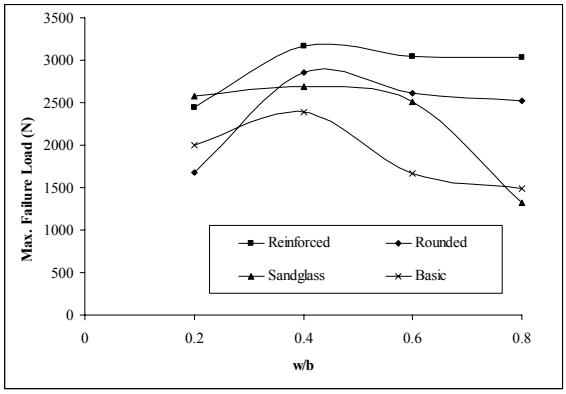

Fig. 16. The changes in the load-carrying capacities of the improved butterfly coupling components.

specimens made with the butterfly coupling components at the (x/w) ratio of 0.2 according to the (w/b) ratios are shown in Fig. 16. The load-carrying capacity depends on the (w/b) ratio, and the load-carrying capacity of all the models was at the maximum at a (w/b) ratio of 0.4. When (w/b) ratio is lower than 0.4, damage occurs mostly on butterfly; however, when it is higher than 0.4, damage occurs on the composite specimen. The highest load-carrying capacity was obtained with the reinforced model. When the specimen was under load in the reinforced model, butterfly coupling component pushed the legs of the specimen on its sides outwardly and by means of the reinforcement rods, the motions of the legs of these specimens were prevented and the load was mostly transmitted over the butterfly. For this reason, maximum load capacity was attained. Butterfly coupling components can be listed from high to low in terms of their load-carrying capacities: reinforced, rounded, sandglass, and basic models.

Fig. 15 illustrates that, according to the data obtained from the experiments, maximum load-carrying capacity was observed with the (x/w) ratio of 0.2 and (w/b) ratio of 0.4 for each model. The stress analysis of the joints made with different butterfly coupling components improved in these geometric ratios is shown in Fig. 17. The stress values from the stress analysis made under the same load were different due to the different butterfly geometries. Maximum stress values were

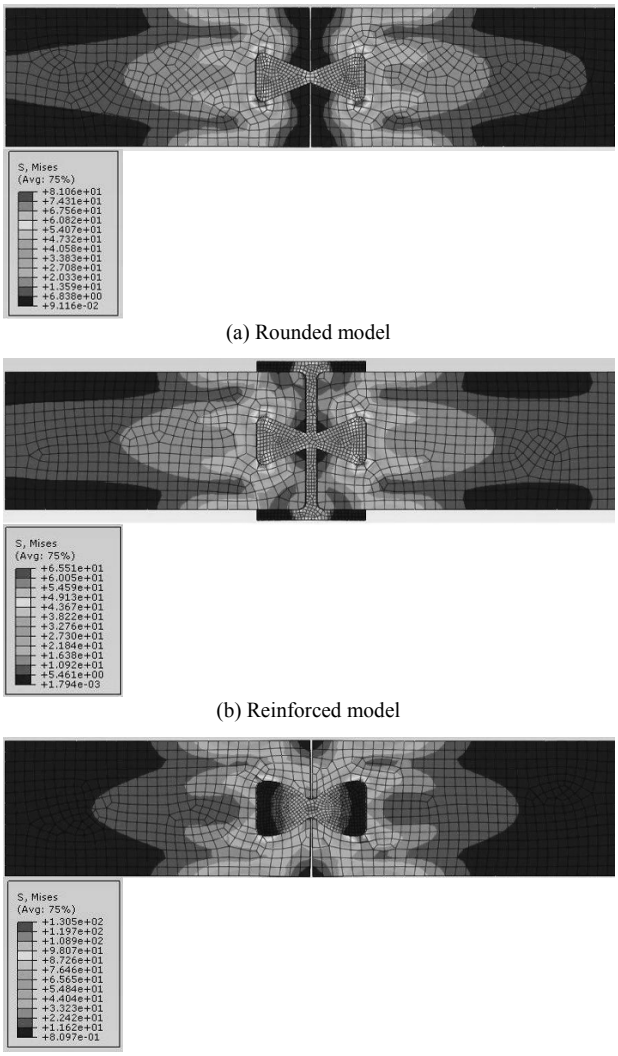

Fig. 17. Stress analysis of the improved butterfly models.

obtained from the joints made with sandglass, rounded, and reinforced model. Thus, it is expected that the joints made with the reinforced model will have the highest load-carrying capacity. These results are in agreement with the results of the experiments.

The stress values that occurred at the fixed ratios of w/b= 0.4 and x/w= 0.2 and along the butterfly axis (Way 1) are shown in Fig. 18. The distribution of the stress occurring on the reinforced butterfly model has a fixed stress value both on the end sides and in the middle parts. In this case, it was determined that the butterfly locked well and that it will have higher damage load than the other models. It was also determined that there were rather low stress values in the end sides of the butterfly coupling component in the sandglass model due to its geometry. The stress values grew in the middle parts of the butterfly coupling component made with the sandglass model. It was determined that the difference between the stress values in the end sides of the rounded butterfly model and the stress values in the middle parts of the rounded butter-

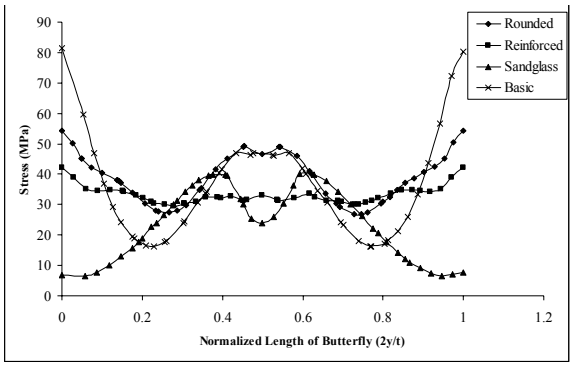

Fig. 18. The comparison of the improved butterfly models.

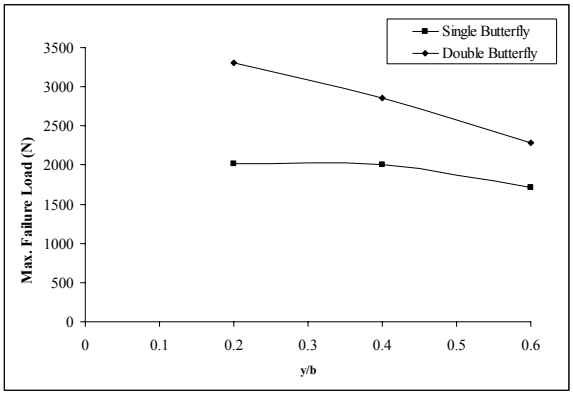

Fig. 19. The comparison of the single and double basic butterfly joints (x/w=0.2).

fly model was less than that of the basic butterfly model. Thus, we can state that the load-carrying capacity obtained from the rounded butterfly model will be much higher than the basic butterfly model.

The changes in the maximum damage of double and single composite basic butterfly model for the different butterfly half-lengths (y/b) in the fixed (x/w) ratio of 0.2 are shown in Fig. 19. Considering the width of the specimen in the double composite basic butterfly model, the butterfly end width (w) was chosen as 8 mm. To compare the load-carrying capacity of the single butterfly joint with that of the double butterfly joint, the end width (w) of butterfly was taken as the same in the experiments. The load-carrying capacity of double butterfly joints was higher than that of single butterfly joints in all the (y/b) ratios. The load-carrying capacities of single and double butterfly joints were higher than those of the other butterfly half-lengths when the ratio of (y/b) was 0.2.

Fig. 20 shows the stress analysis of the single and double butterfly joints made with the half-length of butterfly (y) at 16 mm, butterfly end width (w) at 8 mm, and (x/w) ratio at 0.2. Stress analysis was made under the same load. As seen in Fig. 20, maximum stresses only occurred on the butterfly. When their stress values were compared, it was determined that the stress values occurring on the single butterfly joint were higher than the ones on the double butterfly joint. Thus, the joint made with double butterfly is expected to be damaged

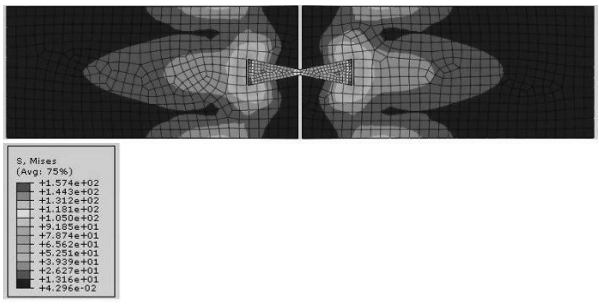

(a) Single butterfly joint

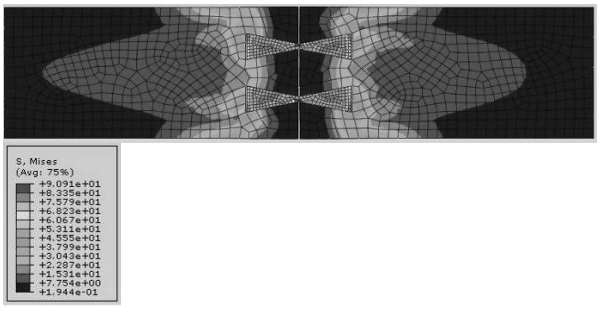

(b) Double butterfly joint

Fig. 20. Stress analysis of single and double butterfly joints.

later than the one with a single butterfly. This result has been confirmed by the results of the experiment.

5. Conclusions

In this study, the effects of the geometric parameters of butterfly-shaped couplings (x/w, y/b and w/b) on their damage loads were analyzed numerically and experimentally. Moreover, by improving the shape of the butterfly coupling component, new load-carrying capacities were also investigated. The following results have been obtained from the experimental and numerical study:

Load-carrying capacities determined from the numerical analysis results conducted with the finite-elements method were confirmed by the results obtained with the experimental method.

It may be an advantage that the damage on the butterfly-shaped couplings can be seen before the composite structure is totally damaged. The service life of the composite structure can be increased with the repair of the butterfly lock.

With the high values of (x/w) ratio, the ratio of butterfly middle width to the butterfly end width, and when the joint load falls and x/w is 1, adhesive joints should be preferred.

It was determined that as the (w/b) ratio increases, its load-carrying capacity decreases. With the increase in the butterfly end width in the specimen at a fixed 'b' width, it was proven experimentally and numerically that load-carrying capacity falls because the specimen was damaged with the weakening of the site in either side of the butterfly coupling component.

It is possible to get different joint load-carrying capacities by changing the shapes of the butterfly coupling components. The models that improved according to the maximum load-

carrying capacity are the reinforced butterfly, rounded butterfly, and sandglass models.

It was found out that the load-carrying capacities of the double butterfly joints made by using the butterfly coupling components of the same geometric properties as those of the single joints are the highest.

Acknowledgements

The authors wish to express their gratitude to the TUBITAK, Turkey, Project No: 106M113 for providing financial support for this study.

References

[1] B. Okutan and R. Karakuzu, The Strength of Pinned Joints in Laminated Composites, Composite Science and Technology, 63 (2003) 893-905.

[2] B. M. Içten, R. Karakuzu and M. E. Toygar, Failure analysis of woven Kevlar fiber reinforced epoxy composites pinned joints, Composite Structures, 73 (2006) 443-450.

[3] S. B. Kumar, I. Sridhar, S. Sivashanker, S. O. Osiyemi and A. Bag, Tensile failure of adhesively bonded CFRP composite scarf joints, Materials Science and Engineering B, 132 (2006) 113-120.

[4] K. Ishii, M. Imanaka, H. Nakayama and H. Kodama, Fatigue failure criterion of adhesively bonded CFRP/metal joints under multiaxial stress conditions, Composites Part A, 29A (1998) 415-422.

[5] J. H. Kim, B. J. Park and Y. W. Han, Evaluation of fatigue characteristics for adhesively-bonded composite stepped lap joint, Composite Structures, 66 (2004) 69-75.

[6] C. Yang, H. Huang, J. S. Tomblin and W. Sun, Elastic-plastic model of adhesive-bonded single-lap composite joints, Journal of Composite Materials, 38 (2004) 293-302.

[7] J. H. Kweon, J. W. Jung, T. H. Kim, J. H. Choi and D. H. Kim, Failure of carbon composite-to-aluminum joints with combined mechanical fastening and adhesive bonding, Composite Structures, 75 (2006) 192-198.

[8] L. F. M. Silva and R. D. Adams, Techniques to reduce the peel stresses in adhesive joints with composites, International Journal of Adhesion and Adhesives, 27 (2007) 227-235.

[9] G. P. Zou, K. Shahin and F. Taheri, An analytical solution for the analysis of symmetric composite adhesively bonded joints, Composite Structures, 65 (2004) 499-510.

[10] Loctite Global Design Handbook, Loctite European Group, Germany.

[11] Y. A. Bahei-El-Din and G. J. Dvorak, New Designs of adhesive joints for thick composite laminates, Composite Science and Technology, 61 (2001) 19-40.

[12] M. Grassi, B. Cox and X. Zhang, Simulation of pin-reinforced single-lap composite joints, Composite Science and Technology, 66 (2006) 1623-1638.

[13] A. Aktas and M. H. Dirikolu, An experimental and numerical investigation of strength characteristics of carbon-epoxy pinned-joint plates, Composite Science and Technology, 64 (2004) 1605-1611.

[14] Q. Zeng and C. T. Sun, Fatigue performance of a bonded wavy composite lap joint, Fatigue&Fracture Engineering Materials&Structures, 27 (2004) 413-422.

[15] ASTM D 3039/D 3039M-00, Standard Test Method for Tensile Properties of Polymer Matrix Composite Materials, American Institute.

[16] ASTM D 3410-75, Standard Test Method for Compressive Properties of Unidirectional or Cross ply Fiber-Resin Composites, American Institute.

[17] R. F. Gibson, Principles of Composite Material Mechanics, McGraw-Hill Company, Singapore, (1994).

[18] ASTM D 5379/D 5379M – 98, Standard Test Method for Shear Properties of Composite Materials by the V-Notched Beam Method, American Institute.

[19] ASTM D 3518-76, Standard Recommended Practice for in plane Shear Stress-Strain Response of Unidirectional Reinforced Plastics, American Institute.

[20] R. M. Jones, Mechanics of Composite Material, McGraw-Hill Company, Kogakusha, Tokyo, (1975).

[21] M. Topçu, G. Altan and E. Ergun, An experimental investigation on damage loads of butterfly joints in composite structures, Advanced Composite Letters 16 (6) (2007) 197-204.

Gürkan Altan is a Research Assistant of Mechanical Engineering at the University of Pamukkale, Denizli, Turkey. Gürkan Altan received his B.E. degree in Mechanical Engineering from Dokuz Eylül University, Izmir, in 1999. He received his M.S. and Ph.D. degrees in Mechanical Engineering from Pamukkale University, Denizli, in 2004 and 2009, respectively. Dr. Altan is interested in the production and applications of composite materials. He is currently involved in the development and application of joints of composite structures.